Engineering of Zeno dynamics in integrated photonics

Quancheng Liu, Weijie Liu, Klaus Ziegler, Feng Chen

Angaben zur Veröffentlichung / Publication details:

Liu, Quancheng, Weijie Liu, Klaus Ziegler, and Feng Chen. 2023. "Engineering of Zeno dynamics in integrated photonics." *Physical Review Letters* 130 (10): 103801. https://doi.org/10.1103/physrevlett.130.103801.

Engineering of Zeno Dynamics in Integrated Photonics

Quancheng Liu,[1,2,*] Weijie Liu,[1,*] Klaus Ziegler,[3] and Feng Chen[1,†]
[1]School of Physics, State Key Laboratory of Crystal Materials, Shandong University, Jinan 250100, China
[2]Department of Physics, Institute of Nanotechnology and Advanced Materials, Bar-Ilan University, Ramat-Gan 52900, Israel
[3]Institut für Physik, Universität Augsburg, D-86135 Augsburg, Germany

(Received 23 June 2022; revised 6 November 2022; accepted 15 February 2023; published 10 March 2023)

Frequent observations to a quantum system modify its coherent evolution through the Zeno effect and Zeno dynamics. Generally, the measurement process destroys the evolution environment of the monitored system, making repeated observations remain a challenge. Here, using the quantum analogy experiments, we realize and engineer the Zeno effect and Zeno dynamics in optical waveguide arrays, where the optical modes correspond to distinct quantum states, and the temporal evolution is mapped into the spatial propagation. We propose a new, extensible experimental strategy for realizing an optical analog of stroboscopic measurements, which are performed by the build-in, on-demand segmented waveguide portions. The weak-to-strong stroboscopic measurements are realized, where the monitored system undergoes a transition from free evolution to optical Zeno freezing. Setting the measurements in the strong regime, the optical Zeno effect and optical Zeno dynamics are successfully generated, and their relationship is demonstrated in optics. We then propose a novel quantum Zeno slicing approach, which allows us to dynamically engineer the Hilbert space of the monitored system. This generic approach is verified by generating a series of Zeno subspaces with different measurement projectors, based on the quantum-optical analogy. The complexity of light dynamics is largely increased, providing full control of the propagation via steering Zeno dynamics. Our results pave the way for manipulation of quantum states by harnessing Zeno dynamics in integrated photonics.

DOI: 10.1103/PhysRevLett.130.103801

The measurement can change the state of a quantum system. Frequently checking if a quantum system is still in the initial state blocks its coherent evolution to other states, which is known as the Zeno effect or quantum Zeno effect [1–8]. This is analogous to the counterintuitive conception that a flying arrow does not move under watching in the classical world. This effect can be used, for example, to protect the coherence of an unstable system since the decay of a quantum unstable system is quadratic at short times in contrast to the exponential law for the classical case. Repeatedly bringing the system back to the initial state by measurements prolongs its lifetime [9]. However, a quantum Zeno effect does not necessarily imply a freeze-out process. More interestingly, Zeno dynamics or quantum Zeno dynamics refers to the restriction of the quantum evolution to a subspace of the system's Hilbert space, in which frequent measurements set a border on the evolution space, leading to the system propagating in a subspace characterized by measurements [10–13]. So far, Zeno dynamics has been experimentally observed in different physical systems, such as Bose-Einstein condensates [14], Rydberg atoms [15], nitrogen-vacancy centers [16], and cavity quantum electrodynamics [17,18].

Photonics is featured with versatile behaviors of light, providing new possibilities for exploring diverse responses from quantum systems [19–23]. Photonic lattices consisting of evanescently coupled waveguide arrays could be defined as appropriate configurations, in which the optical modes can be engineered along the transverse direction. Particularly, the periodically segmented waveguide is investigated both for a single waveguide [24,25] and in the array [26], which is used for image reconstruction [27], optical lens [28], and generating controllable loss [29]. Because of the analogy of the Schrödinger equation for quantum wave functions and the paraxial Helmholtz equation for classical electric fields, the temporal evolution of a quantum system is therefore equivalent to spatial propagation of guided light waves in waveguides [30,31]. This time-to-space analogy has triggered a reliable method to study various intricate phenomena in physics [32–36]. Particularly, Dreisow *et al.* reported on the experimental demonstration of the optical Zeno effect (OZE) [5,37,38], and Crespi *et al.* investigated quantum decay of guided modes to continuum in optical waveguide arrays [39].

These works demonstrate the practical observations of various Zeno phenomena. Nevertheless, the time-dependent engineering of the Zeno process remains unexplored. This requires new approaches for realizing stroboscopic measurements and advances for dynamical Zeno control. In this Letter, using femtosecond laser direct writing of glass wafer [40,41], we construct specific optical waveguide arrays, which are composed of straight waveguides accompanied with a series of periodic segmented portions. The segmented waveguides induce tailored

periodic modification to the guided light fields, resembling the repeated measurements of the monitored system. The OZE and optical Zeno dynamics (OZD) are realized in the strong measurements regime, generated by relatively long waveguide segments. Based on that, we then design different measurement projectors to engineer the Zeno dynamics, which dynamically "slices" the Hilbert space of the monitored system into multiple Zeno subspaces. This dynamical Zeno control by steering Zeno dynamics is verified in optics, where the resultant laser beam propagates in the predetermined path as we designed.

In the waveguide array, there are refractive index modulations (Δn) in the transverse directions of x and y, and the guided monochromatic light propagates along z orientation. The modulation Δn is much smaller than the substrate refractive index n_0, and the weakly guided propagation of the optical waves follows the Schrödinger-type paraxial wave equation [30,31]

$$i\frac{\partial\Psi(x,y;z)}{\partial z}=\left[-\frac{1}{2k}\nabla_{\perp}^{2}-\frac{k}{n_0}\Delta n(x,y;z)\right]\Psi(x,y;z), \quad (1)$$

where $\nabla_{\perp}^{2}=\partial^2/\partial^2 x+\partial^2/\partial^2 y$, Ψ is the light field envelope of wavelength λ, and $k=2\pi n_0/\lambda$ is the corresponding wave number. Equation (1) formally equals the Schrödinger equation when $z\to t$ and $-\Delta n\to V$. So the light propagation in the waveguide array resembles the evolution of a quantum particle and the desired dynamics can be designed by tuning the modulation Δn. We use the femtosecond laser direct writing to fabricate single-mode waveguide structures for the experiments (Supplemental Material [42]). The crucial point in our work is the implementation of stroboscopic measurements using specially fabricated waveguide portions, which make frequent snapshots on the monitored system.

In our scheme [Fig. 1(a)], we use two continuous waveguides (labeled by WG1 and WG2) with mutual coupling representing a two-level system under monitoring. A periodically segmented waveguide [26,29] is appended to the left side of WG1 at $d=5$ μm, which leads to equivalently stroboscopic measurements on $\mathcal{S}$. For each element of the noncontinuous waveguide, the waveguide segment has the length m, and the segment-to-segment gap is $l-m$. These segmented waveguides serve as the measurement apparatus $\mathcal{M}$, which is coupled to $\mathcal{S}$. In the gap, the coupling between $\mathcal{M}$ and $\mathcal{S}$ vanishes. The light dissipates from $\mathcal{M}$, in which photons are emitted (Supplemental Material [42]). Physically, this process is considered as the readout, even if the emitted photons are not detected [14]. Depending on the relative lengths of the segmented waveguide m and gap $l-m$, we define two distinct regimes, i.e., the weak measurement limit when $m\ll l-m$ and the strong measurement limit when $m\gg l-m$. In the experiment, we perform total $N=60$ measurements (60 portions) in the time interval $t=T/2$,

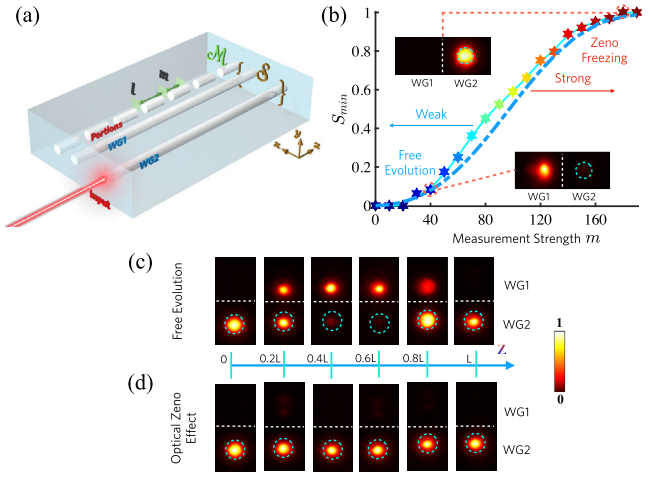

FIG. 1. Measurements protocol and optical Zeno effect. (a) Illustration of the measurement protocol $\mathcal{M}$ for a two-level system $\mathcal{S}$ using segmented waveguide portions. (b) Measured survival probability $S_{\min}$ versus the measurement strength m. For each m, we fabricate a group of waveguide arrays and measure the light intensity for different propagation lengths of step 0.5 mm (total propagation length is 12 mm, Supplemental Material [42]) then find $S_{\min}$. We fabricate 20 groups waveguide arrays corresponding to 20 ms. When m is small, the light deviates from its initial state and $S_{\min}\to 0$. In the strong measurement regime, we observe the Zeno effect, where $S_{\min}\to 1$, indicating freezing the light on WG2. The blue dashed line is given by coupled mode equations, where the segmented waveguide is mapped to an effective straight waveguide with the refractive index given by $\Delta n_{\text{effective}}=m\Delta n/l$. (c),(d) Measured light distribution on WG1 and WG2 versus the distance z without measurements (c) and at Zeno limit (d).

where T is the Rabi oscillation period of $\mathcal{S}$. We use a classical 633 nm He-Ne laser to excite the system from WG2, and measure the light survival probability on WG2. It has been well accepted that light mode evolution via single-photon excitation follows the same behaviors as the classic light case in waveguide arrays [40,44–46]. The minimal survival probability $S_{\min}=\min[S(t)]=\min(|\langle\psi_0|\psi(t)\rangle|^2)$, $t\in[0,T/2]$ is to characterize the magnitude of the backaction from measurements. As depicted in Fig. 1(b), the experimental $S_{\min}$ increases as the measurement strength is enlarged. There is a crossover in the survival probability, after which $S_{\min}\to 1$, suggesting that the system is frozen in its initial state (A coupled-mode theory explanation is shown in [42]). This is the observation of the optical analogy of the Zeno effect by the "measurement" from the waveguide portions, which suppresses the tunneling between the WG1 and WG2. We present the measured light distribution of WG1 and WG2 as a function of propagation length z for free evolution in Fig. 1(c) and strong measurements ($N=120$ measurements) in Fig. 1(d), where $\mathcal{S}$ undergoes a transition from free oscillation to measurement-induced optical Zeno freezing. These results clearly show that the waveguide

portions provide controllable measurements of the system, and generate the OZE in a certain regime.

The above experimental strategy can be extended to the implementation of the Zeno dynamics using this optical-quantum analogy. In the literature, it is supposed that the Zeno effect is a special case of Zeno dynamics [10,47]. As additional freedom is added to the Zeno effect, the system evolves further rather than stops on its initial state. Here we provide an optical demonstration of this hypothesis and report the first realization of the OZD. This is achieved by utilizing the same arrangement in Fig. 1(a) while adding further freedom in the Zeno subspace via coupling a third waveguide to $\mathcal{S}$ [Fig. 2(a)]. The Hamiltonian of $\mathcal{S}$ reads $H_s = \Omega(|1\rangle\langle 2| + |2\rangle\langle 3| + \text{H.c.})$. We append the similar segmented waveguide portions as in Fig. 1(a) to the WG1 and the number of measurements is 120. The resulting Zeno subspace then changes from $H_p = |2\rangle\langle 2|$ for the system with two waveguides coupled to measurements [Fig. 1(a)] to $H_p = \Omega(|2\rangle\langle 3| + |3\rangle\langle 2|)$ when we have three waveguides [Fig. 2(a)]. Different from the freezing effect in Fig. 1(d), the experimental results here confirm the theoretical prediction [Fig. 2(c)], i.e., the light exhibits a Rabi oscillation characterized by the new Zeno subspace H_p [Fig. 2(e)]. This also differs from the original three-level dynamics of H_s [Figs. 2(b) and 2(d)], since the tunneling between WG1 and WG2 is inhibited by the waveguide portions. To conclude, we observe the OZD confined in the Zeno subspace and present an optical verification of the relationship between the Zeno effect and Zeno dynamics.

The above two experiments demonstrate practical solutions to generate the Zeno phenomena in optics using the segmented waveguide. In what follows, we propose a theoretical formalism for implementing universal quantum control with Zeno dynamics using the quantum "Zeno slicing" approach. The strategy is to dynamically slice the system's Hilbert space with Zeno dynamics by properly engineering the measurements, resulting in a series of noncommutative Zeno subspaces. The complexity of the resultant quantum dynamics largely raises, far beyond its original evolution control by H_s or by the single Zeno subspace H_p, enabling the full control of the monitored $\mathcal{S}$. The evolution now reads (Supplemental Material [42])

$$\rho(t) = e^{-iH_p^n \delta t_n} \cdots e^{-iH_p^1 \delta t_1} \rho_0 e^{iH_p^1 \delta t_1} \cdots e^{iH_p^n \delta t_n}, \quad (2)$$

where $H_p^i = P_i H_s P_i$ is the Zeno subspace, and P_i is the measurement projector (i.e., the measured states $P_i = \sum |d\rangle\langle d|$) determined by the ith Zeno measurements. δt_i is the evolution time in subspace H_p^i, controlled by the number of the segmented portions, which ensures $\mathrm{Tr}[\rho(t+\delta t_i)P_{i+1}] = \mathrm{Tr}[\rho(t+\delta t_i)H_p^{i+1}] = 1$ with suitable choices. Now the system $\mathcal{S}$ evolves unitarily under arbitrary transformations controlled by e^{Θ}, where Θ is an anti-Hermitian operator given by the Lie group $\mathfrak{L}_{\text{zeno}} = \mathfrak{Lie}\{iH, iH_p^1, iH_p^2, \ldots, iH_p^n\}$. This guarantees that all the required transformations on the system can be generated by different Zeno measurements, and hence it can be fully controlled via engineering the Zeno dynamics.

We demonstrate experimentally the Zeno control in the optical waveguide array by dynamically tailoring the Hilbert space of a five-site optical lattice using Zeno slicing. The array consisting of channels from WG1 to WG5 represents a photonic lattice under monitoring [Fig. 3(a)]. The Zeno measurements are performed by the six groups of segmented waveguides (each group contains $N = 60$ portions) that are fabricated above the photonic lattice [Figs. 3(a) and 3(c)].

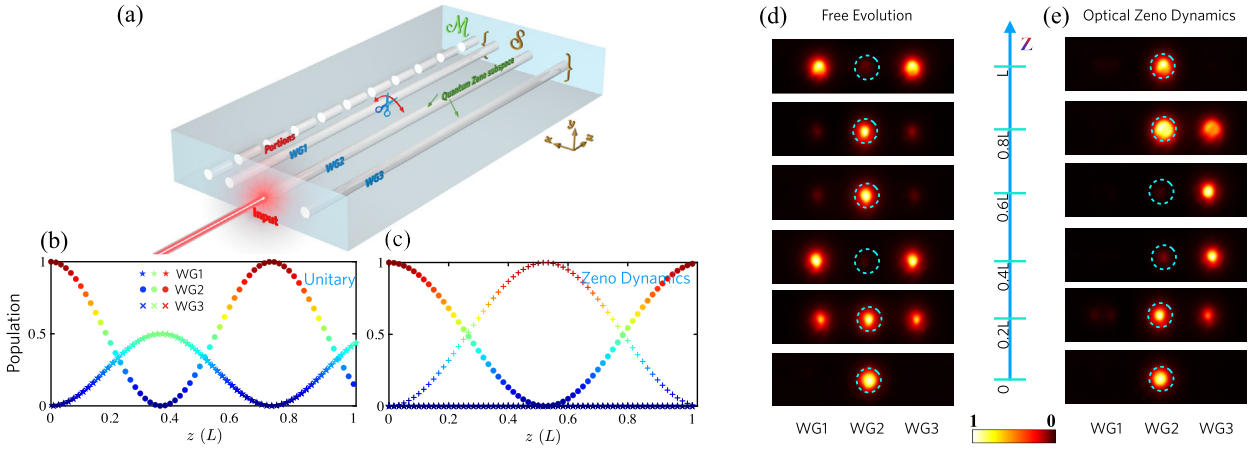

FIG. 2. Optical Zeno dynamics. (a) Schematic diagram of the monitored system $\mathcal{S}$ and measurements $\mathcal{M}$. (b),(c) The theoretical population distribution on the continuous waveguides versus z for free evolution (b) and Zeno dynamics (c). (d) Experimental light distribution on continuous waveguides for free evolution (b). (e) Experimental light distribution for continuous waveguides under strong measurements. Now the light can only tunnel between WG2 and WG3 (c), and the hopping between WG1 and WG2 is inhibited by the waveguide portions.

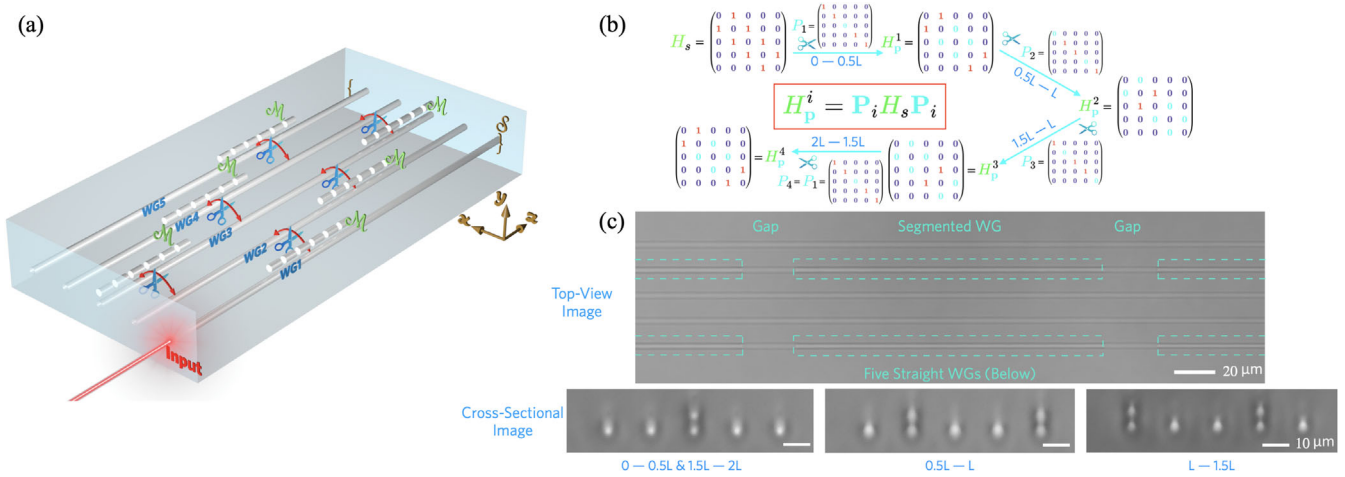

FIG. 3. Zeno slicing. (a) Schematic illustration of the dynamical control to a five-site tight-binding lattice $\mathcal{S}$ using Zeno slicing. The lattice $\mathcal{S}$ is simulated by the continuous waveguide array (below). On its top, we apply six different groups of waveguide portions to generate OZD (total 360 portions), which slices the Hilbert space of $\mathcal{S}$ into different Zeno subspaces. (b) The engineered Hamiltonian H_p^i of $\mathcal{S}$ by quantum Zeno slicing. The propagation of the light on the waveguide array is restricted in the Zeno subspace H_p^i in the time-distance $(i-1)T/2 \sim iT/2$. (c) Experimental micrograph of facets of the fabricated waveguide array and noncontinuous portions.

These engineer the Hamiltonian of the photonic lattice and generate four different Zeno subspaces [Fig. 3(b)]. The system is excited from the WG1. Physically, this could be considered as a continuous-time quantum walk on a tight-binding lattice [48,49]. We calculate the population distribution on the waveguide array for a unitary evolution [Fig. 4(a)] and Zeno measurements [Fig. 4(b)]. Instead of spreading to all the lattice nodes [Fig. 4(a)], the quantum walk controlled by Zeno slicing is monodirectional. It visits the lattice nodes from the right to the left with probability unity at specific times [Fig. 4(b)]. This node-to-node propagation is perfectly measured in the experiment [Figs. 4(b) and 4(d)].

Specifically, at the length regime $z = 0 \sim 0.5L$, 60 portions are coupled to WG3 [Fig. 3(a)], leading to the measurement projector $P_1 = I - |3\rangle\langle 3|$ (I is the identity matrix). The corresponding Zeno subspace $H_p^1 = P_1 H_s P_1 = \Omega(|1\rangle\langle 2| + |4\rangle\langle 5| + \text{H.c.})$ [Fig. 3(b)], where the lattice is divided into two localized subsystems. Since the system is excited from WG1, the light propagates in the right

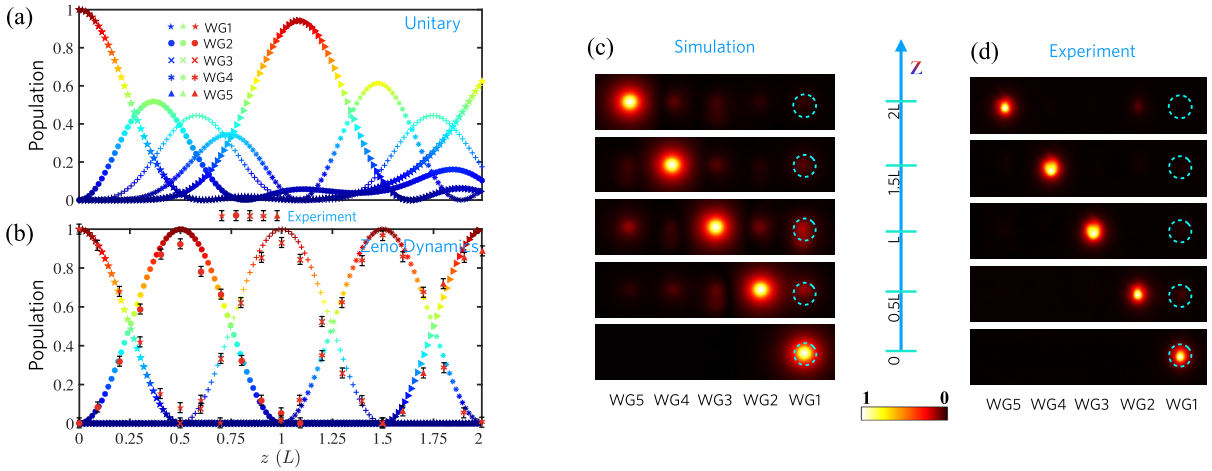

FIG. 4. Node-to-node mono-directional quantum walk in the optical lattice. (a) The light distribution on the waveguide array versus the propagation distance z without measurements (unitary evolution). (b) Experimental and theoretical [Eq. (2)] light distribution on waveguides when the array is steered by the Zeno slicing. Now the light determinately jumps from the right waveguide to the left one and localizes only on the ith waveguide at distance $(i-1)L/2$. The spread to the whole array (a) is inhibited by the waveguide portions, which proves the Zeno control in optics using the slicing approach. (c) Simulated light intensity distribution in the waveguide array (with portions) based on the beam propagation method. (d) Experimental picture of the node-to-node quantum walk, where the walker deterministically arrives at each node with probability unity at specific times, as Eq. (2) predicted.

subsystem with $e^{-iH_p^1\delta t_1}\rho_0 e^{iH_p^1\delta t_1}$, which deterministically hops from WG1 to WG2 at $z = 0.5L$ [Figs. 4(b) and 4(d)]. We then couple $\mathcal{M}$ to WG1 and WG4 in $0.5L \sim L$ [Fig. 3(a)], which leads to the projector $P_2 = |2\rangle\langle 2| + |3\rangle\langle 3| + |5\rangle\langle 5|$. Consequently, the walker is restricted to jump only between the WG2 and WG3, in the subspace $H_p^2 = P_2 H_s P_2 = \Omega(|2\rangle\langle 3| + |3\rangle\langle 2|)$ [Fig. 3(b)]. And the walker reaches WG3 at $z = L$ [Figs. 4(b) and 4(d)], where the $\mathcal{M}$ changes again. In the third setup, the measurement apparatus is coupled to the WG2 and WG5 in the spatial regime of $z = L \sim 1.5L$. We have $H_p^3 = \Omega(|3\rangle\langle 4| + |4\rangle\langle 3|)$, and the walker localizes on the WG4 at $1.5L$ [Figs. 4(b) and 4(d)]. In the last Zeno slicing, $\mathcal{M}$ is coupled to WG3 again, hence $P_4 = P_1$ and $H_p^4 = H_p^1$. Now the walker evolves in the left subsystem, and it reaches WG5 with probability one at $z = 2L$ [Fig. 4(d)]. The measured light dynamics [Fig. 4(b)] are in full accordance with our theoretical predictions from Eq. (2), confirming the practical quantum control by engineering the Zeno dynamics.

In summary, we have demonstrated the experimental realization of the OZE and OZD in photonics, using the on-demand periodically segmented waveguides. By precisely changing the length of the waveguide portions, we realize the weak-to-strong transition of repeated measurements, where the system undergoes a free evolution to optical Zeno freezing. These optical-quantum analogy experiments indicate that the Zeno effect is rooted in the strong interactions between the system and measurement apparatus. A proof of the relationship between the Zeno effect and Zeno dynamics is provided from optics, indicating that the former is a special case of the latter. Physically, these results also provide a deeper understanding of the Zeno effect and Zeno dynamics, and more fundamentally, the basic concept of quantum measurement.

The highlight of this work is the universal quantum control using Zeno slicing. For the first time, we show that the Zeno dynamics could be a versatile tool for the control and manipulation of the monitored system through time-dependent Hilbert space engineering. This enables the Zeno dynamics from an exotic physical phenomenon, becoming a technical method for quantum control and quantum information processing. The experimental approach for the implementation of Zeno control may be used to pause the photonic state evolution for a flexible length of time via suitable segmented waveguides, for example, in quantum walks. Other potential applications may include dynamic modification of system evolution, preparation of specific system states, and controlling the transport in system. Our work opens the gate for more advanced quantum controls using Zeno steering approaches and experimental tools.

We are grateful to Eli Barkai and Zongquan Zhou for helpful discussions. This work was supported by National Natural Science Foundation of China (Grant No. 12174222), Natural Science Foundation of Shandong Province (Grant No. ZR2021ZD02), and Taishan Scholars Program (tspd20210303).The support of Israel Science Foundation's grant 1614/21 is acknowledged. K. Z. acknowledges support from Julian Schwinger Foundation for Physics Research.

*Q. L. and W. L. contributed equally to this work.
†Corresponding author.
drfchen@sdu.edu.cn

[1] B. Misra and E. C. G. Sudarshan, J. Math. Phys. (N.Y.) **18**, 756 (1977).
[2] W. M. Itano, D. J. Heinzen, J. J. Bollinger, and D. J. Wineland, Phys. Rev. A **41**, 2295 (1990).
[3] P. Facchi, H. Nakazato, and S. Pascazio, Phys. Rev. Lett. **86**, 2699 (2001).
[4] E. W. Streed, J. Mun, M. Boyd, G. K. Campbell, P. Medley, W. Ketterle, and D. E. Pritchard, Phys. Rev. Lett. **97**, 260402 (2006).
[5] F. Dreisow, A. Szameit, M. Heinrich, T. Pertsch, S. Nolte, A. Tünnermann, and S. Longhi, Phys. Rev. Lett. **101**, 143602 (2008).
[6] Y. S. Patil, S. Chakram, and M. Vengalattore, Phys. Rev. Lett. **115**, 140402 (2015).
[7] S. Hacohen-Gourgy, L. P. García-Pintos, L. S. Martin, J. Dressel, and I. Siddiqi, Phys. Rev. Lett. **120**, 020505 (2018).
[8] W. Ren, W. Liu, C. Song, H. Li, Q. Guo, Z. Wang, D. Zheng, G. S. Agarwal, M. O. Scully, S. Y. Zhu, H. Wang, and D. W. Wang, Phys. Rev. Lett. **125**, 133601 (2020).
[9] P. M. Harrington, J. T. Monroe, and K. W. Murch, Phys. Rev. Lett. **118**, 240401 (2017).
[10] P. Facchi and S. Pascazio, J. Phys. A **41**, 493001 (2008).
[11] A. Smerzi, Phys. Rev. Lett. **109**, 150410 (2012).
[12] D. K. Burgarth, P. Facchi, V. Giovannetti, H. Nakazato, S. Pascazio, and K. Yuasa, Nat. Commun. **5**, 5173 (2014).
[13] Y. Lin, J. P. Gaebler, F. Reiter, T. R. Tan, R. Bowler, Y. Wan, A. Keith, E. Knill, S. Glancy, K. Coakley, A. S. Sørensen, D. Leibfried, and D. J. Wineland, Phys. Rev. Lett. **117**, 140502 (2016).
[14] F. Schäfer, I. Herrera, S. Cherukattil, C. Lovecchio, F. Cataliotti, F. Caruso, and A. Smerzi, Nat. Commun. **5**, 3194 (2014).
[15] A. Signoles, A. Facon, D. Grosso, I. Dotsenko, S. Haroche, J.-M. Raimond, M. Brune, and S. Gleyzes, Nat. Phys. **10**, 715 (2014).
[16] N. Kalb, J. Cramer, D. J. Twitchen, M. Markham, R. Hanson, and T. H. Taminiau, Nat. Commun. **7**, 13111 (2016).
[17] J. M. Raimond, C. Sayrin, S. Gleyzes, I. Dotsenko, M. Brune, S. Haroche, P. Facchi, and S. Pascazio, Phys. Rev. Lett. **105**, 213601 (2010).
[18] G. Barontini, L. Hohmann, F. Haas, J. Estève, and J. Reichel, Science **349**, 1317 (2015).
[19] A. Regensburger, C. Bersch, M.-A. Miri, G. Onishchukov, D. N. Christodoulides, and U. Peschel, Nature (London) **488**, 167 (2012).
[20] M.-A. Miri and A. Alù, Science **363**, eaar7709 (2019).

[21] R. El-Ganainy, K. G. Makris, M. Khajavikhan, Z. H. Musslimani, S. Rotter, and D. N. Christodoulides, Nat. Phys. **14**, 11 (2018).
[22] H. Tang, T.-Y. Wang, Z.-Y. Shi, Z. Feng, Y. Wang, X.-W. Shang, J. Gao, Z.-Q. Jiao, Z.-M. Li, Y.-J. Chang, W.-H. Zhou, Y.-H. Lu, Y.-L. Yang, R.-J. Ren, L.-F. Qiao, and X.-M. Jin, Photonics Res. **10**, 1430 (2022).
[23] Y.-K. Sun, X.-L. Zhang, F. Yu, Z.-N. Tian, Q.-D. Chen, and H.-B. Sun, Nat. Phys. **18**, 1080 (2022).
[24] Z. Weissman and A. Hardy, J. Lightwave Technol. **11**, 1831 (1993).
[25] L. Li and J. J. Burke, Opt. Lett. **17**, 1195 (1992).
[26] C. Minot, J. M. Moison, S. Guilet, E. Cambril, A. Levenson, and N. Belabas, Opt. Lett. **42**, 539 (2017).
[27] A. Szameit, F. Dreisow, M. Heinrich, T. Pertsch, S. Nolte, A. Tünnermann, E. Suran, F. Louradour, A. Barthélémy, and S. Longhi, Appl. Phys. Lett. **93**, 181109 (2008).
[28] N. Matsushima, Jpn. J. Appl. Phys. **54**, 052501 (2015).
[29] S. Xia, D. Kaltsas, D. Song, I. Komis, J. Xu, A. Szameit, H. Buljan, K. G. Makris, and Z. Chen, Science **372**, 72 (2021).
[30] S. Longhi, Laser Photonics Rev. **3**, 243 (2009).
[31] M. Segev, Y. Silberberg, and D. N. Christodoulides, Nat. Photonics **7**, 197 (2013).
[32] M. C. Rechtsman, J. M. Zeuner, Y. Plotnik, Y. Lumer, D. Podolsky, F. Dreisow, S. Nolte, M. Segev, and A. Szameit, Nature (London) **496**, 196 (2013).
[33] O. Zilberberg, S. Huang, J. Guglielmon, M. Wang, K. P. Chen, Y. E. Kraus, and M. C. Rechtsman, Nature (London) **553**, 59 (2018).
[34] N. Tischler, C. Rockstuhl, and K. Słowik, Phys. Rev. X **8**, 021017 (2018).
[35] M. Ehrhardt, M. Heinrich, and A. Szameit, Nat. Photonics **16**, 191 (2022).
[36] T. Ozawa, H. M. Price, A. Amo, N. Goldman, M. Hafezi, L. Lu, M. C. Rechtsman, D. Schuster, J. Simon, O. Zilberberg, and I. Carusotto, Rev. Mod. Phys. **91**, 015006 (2019).
[37] S. Longhi, Phys. Rev. Lett. **97**, 110402 (2006).
[38] P. Biagioni, G. D. Valle, M. Ornigotti, M. Finazzi, L. Duò, P. Laporta, and S. Longhi, Opt. Express **16**, 3762 (2008).
[39] A. Crespi, F. V. Pepe, P. Facchi, F. Sciarrino, P. Mataloni, H. Nakazato, S. Pascazio, and R. Osellame, Phys. Rev. Lett. **122**, 130401 (2019).
[40] A. Szameit and S. Nolte, J. Phys. B **43**, 163001 (2010).
[41] F. Chen and J. R. V. de Aldana, Laser Photonics Rev. **8**, 251 (2014).
[42] See Supplemental Material at http://link.aps.org/supplemental/10.1103/PhysRevLett.130.103801 for further experimental, analytical, and numerical details, which includes Ref. [43].
[43] V. Dubey, C. Bernardin, and A. Dhar, Phys. Rev. A **103**, 032221 (2021).
[44] F. Lederer, G. I. Stegeman, D. N. Christodoulides, G. Assanto, M. Segev, and Y. Silberberg, Phys. Rep. **463**, 1 (2008).
[45] H. Tang, C. Di Franco, Z.-Y. Shi, T.-S. He, Z. Feng, J. Gao, K. Sun, Z.-M. Li, Z.-Q. Jiao, T.-Y. Wang, M. S. Kim, and X.-M. Jin, Nat. Photonics **12**, 754 (2018).
[46] X.-L. Zhang, F. Yu, Z.-G. Chen, Z.-N. Tian, Q.-D. Chen, H.-B. Sun, and G. Ma, Nat. Photonics **16**, 390 (2022).
[47] P. Facchi and S. Pascazio, Phys. Rev. Lett. **89**, 080401 (2002).
[48] X.-Y. Xu, X.-W. Wang, D.-Y. Chen, C. M. Smith, and X.-M. Jin, Nat. Photonics **15**, 703 (2021).
[49] H. B. Perets, Y. Lahini, F. Pozzi, M. Sorel, R. Morandotti, and Y. Silberberg, Phys. Rev. Lett. **100**, 170506 (2008).